

Ridge from strings

M.A.Braun^a, C.Pajares^b, V.V.Vechernin^a

^a Dep. of High Energy physics, Saint-Petersburg State University, Russia

^b Dep. of Particles, University of Santiago de Compostela, Spain

July 18, 2014

Abstract In the colour string picture with fusion and percolation it is shown that long range azimuthal-rapidity correlations (ridge) can arise from the superposition of many events with exchange of clusters of different number of strings and not from a single event. Relation of the ridge with the flow harmonics coefficients is derived. By direct Monte-Carlo simulations, in the technique previously used to calculate these coefficients, ridge correlations are calculated for AA, pA and pp collisions. The azimuthal anisotropy follows from the assumed quenching of the emitted particles in the strong colour fields inside string clusters. It is confirmed that in pp collisions the ridge structure only appears in rare events with abnormally high multiplicity. Comparison with the experimental data shows a good agreement. Also a good agreement is found for pPb collisions. For AA collisions a reasonable agreement is found for both near-side and away-side angular correlations although it worsens at intermediate angles.

1 Introduction

One of the most impressive discoveries at LHC is observation of strong long-range rapidity y correlations collimated at small relative azimuthal angles ϕ in particle production in proton-proton [1] and proton-nucleus collisions [2, 3, 4], the so called "ridge". Before the similar effect was discovered in nucleus-nucleus collisions [5, 6, 7].

Several approaches tried to understand this effect [8]-[17]. Long-range rapidity correlations have been successfully described since long ago (see e.g. [18], [19]). It is more difficult to explain mixed rapidity-azimuthal angle correlations. In the Colour-Glass Condensate approach to explain it specific diagrams were studied corresponding to subdominant contributions at large number of colours which may generate such y, ϕ correlations [8]-[13]. In this approach ridge is related to correlations at initial stages of particle production and is a property of basic emission process, which is then translated in the observable picture by the hydrodynamic flow. In [17] the color field is assumed to be distributed in domains in the transverse plane, the direction the field different in different domains. Partons interacting with each domain remember this direction, which is the reason of angular anisotropy.

In this paper we study correlations in the colour string approach. Colour strings picture has been able to successfully explain many observable phenomena in the soft dynamics domain. One expects it to be also applicable to the ridge problem in so far as one is dealing with relatively modest transverse momenta. One of the main advantage of the colour string model is that it allows to consider both AA and proton-proton collisions on the same footing [20] and so gives a unified picture for the ridge in different processes.

Existence of long-range rapidity correlations has long been known in this model and was, in fact, one of its most spectacular predictions. However in the previous simple string models azimuthal dependence was not generated, so that the arising correlations were flat in ϕ . Recently a modification of the colour string model was proposed in which azimuthal dependence is included on the event-by-event basis [21, 22]. This gives some hope to find ridge in the colour string picture. Here we demonstrate that this hope is correct: we calculate the y, ϕ correlations in the framework of [22] and show that they indeed have the ridge form. Note that similar findings were earlier reported in [23] in a simplified analytical approach.

Note that, unlike [11, 12], in the string approach correlations follow not from the basic emission process in a single event but rather from the distribution of events in actual observations. In principle emission from a single string (and thus in an event) could also lead to non-trivial y, ϕ correlation in the spectra due to recoil effect in the transverse space after the first emission [24]. However we show that this effect is small and fast dying with rapidity distance, so that it cannot lead to long-range rapidity correlations. This point is discussed in section 3 after we briefly discuss our modified string picture, which introduces non-trivial ϕ -dependence on the event-by-event basis in Section 2. Section 4 is devoted to the general discussion of the long rapidity correlations in the colour string picture and serves as an introduction to this problem. Section 5 is devoted to the derivation of the expression for the correlation coefficient in this picture. Section 6 presents our numerical results for AA, pp and pA collisions. Some conclusions are collected in Section 6.

2 String picture

The colour string model was proposed some time ago to describe multiparticle production in the soft region. Its basic ideas can be found in original papers and in a review [25, 26, 27]. Its application to the flow problem was developed in our previous paper [22]. Here we only reproduce the main points necessary to understand the technique. It is assumed that in a high-energy collision between the partons of the participants colour strings are stretched, which may be visualized as a sequence of $q\bar{q}$ pairs created from the vacuum or alternatively as a strong chromoelectric field generated by the participant partons. The strings are assumed to possess a certain finite dimension in the transverse space related to confinement. Each string then breaks down in parts several times until its energy becomes of the order of several GeV and it becomes an observed hadron. The number of strings in the interaction area depends on the total available energy and partonic structure of the colliding particles: it grows with energy and atomic number. When the number of strings is small they occupy a small part of the whole interaction area like drops of liquid at considerable distance from one

another. However when the number of string grows they begin to overlap and fuse giving rise to strings with more colour and covering more space in the interaction area. At a certain critical string density strings begin to fuse forming clusters of the dimension comparable to that of the interaction area (string percolation). The basic assumptions which lie at the basis of the colour string picture are supported by its very successful application to multiparticle production in the soft region. It describes well the multiplicity and transverse momentum distributions and many other details of the particle spectra. The colour string picture has a certain similarity (see [28]) with the saturation (Colour Glass Condensate or Glasma) models, where the dynamics is explained by the classical gluon field stretched between the colliding hadrons. The effective number of independent colour sources in string percolation can be put in correspondence with the number of colour flux tubes in the Glasma. It is found that they indeed have the same energy and number of participants dependence. As a consequence predictions of both approaches for most of the observables are similar.

It is assumed that strings decay into particles ($q\bar{q}$ pairs) by the well-known mechanism for pair creation in a strong electromagnetic field. In its simplest version, the particle distribution at the moment of its production by the string is

$$P(p, \phi) = Ce^{-\frac{p_0^2}{T}}. \quad (1)$$

where p_0 is the particle initial transverse momentum, T is the string tension (up to an irrelevant numerical coefficient) and C is the normalization factor. However, as proposed in [22], p_0 is different from the observed particle momentum p because the particle has to pass through the fused string area and emit gluons on its way out. So in fact in Eq. (1) one has to consider p_0 as a function of p and path length l inside the nuclear overlap: $p_0 = f(p, l(\phi))$ where ϕ is the azimuthal angle. Note that Eq. (1) describes the spectra only at very soft p_0 . To extend its validity to higher momenta one may use the idea that the string tension fluctuates, which transforms the Gaussian distribution into the thermal one [29, 30]:

$$P(p, \phi) = Ce^{-\frac{p_0}{\sqrt{T/2}}}. \quad (2)$$

To describe the energy loss of the parton due to gluon emission one may use the corresponding QED picture for a charged particle moving in the external electromagnetic field [31]. This leads to the the quenching formula [22]

$$p_0(p, l) = p \left(1 + \kappa p^{-1/3} T^{2/3} l \right)^3, \quad (3)$$

with the quenching coefficient κ to be taken from the experimental data. We adjusted κ to give the experimental value for the coefficient v_2 in mid-central Au+Au collisions at 200 GeV, integrated over the transverse momenta.

Of course the possibility to use electrodynamic formulas for the chromodynamic case may raise certain doubts. However in [32] it was found that at least in the $N = 4$ SUSY Yang-Mills case the loss of energy of a coloured charge moving in the external chromodynamic field was given by essentially the same expression as in the QED.

3 Correlations in emissions from a single string

3.1 Invariant production probability

Consider a string stretched between two partons (e.g. quark and diquark) with momenta p_1 and p_2 , $p_1^2 = p_2^2 = 0$. We introduce two orthogonal momenta p and q which form the plane orthogonal to emission momenta:

$$p = p_1 + p_2, \quad q = p_1 - p_2, \quad (pq) = 0.$$

To define the emission probability for a parton of momentum k we introduce momentum \tilde{k} orthogonal to plane p, q

$$\tilde{k} = k - p \frac{(kp)}{p^2} - q \frac{(kq)}{q^2}. \quad (4)$$

We trivially find

$$(p\tilde{k}) = (q\tilde{k}) = 0$$

and

$$\tilde{k}^2 = k^2 - \frac{(kp)^2}{p^2} - \frac{(kq)^2}{q^2}. \quad (5)$$

Let $p_{1\perp} = p_{2\perp} = 0$. Then $p_{1-} = p_{2+} = 0$, so that

$$p_+ = p_{1+}, \quad p_- = p_{2-}, \quad q_+ = p_+, \quad q_- = -p_-$$

and we find

$$\begin{aligned} \tilde{k}_+ &= k_+ - p_+ \frac{k_+ p_- + k_- p_+}{2p_+ p_-} + p_+ \frac{-k_+ p_- + k_- p_+}{2p_+ p_-} = 0, \\ \tilde{k}_- &= k_- - p_- \frac{k_+ p_- + k_- p_+}{2p_+ p_-} - p_- \frac{-k_+ p_- + k_- p_+}{2p_+ p_-} = 0, \\ \tilde{k}_\perp &= k_\perp, \end{aligned}$$

as expected. So we can take for the invariant density (suppressing the normalization factor)

$$\rho(k) = \frac{dW}{dy d^2 k_\perp} = e^{a\tilde{k}^2}, \quad (6)$$

which in the case $p_{1\perp} = p_{2\perp} = 0$ transforms into the standard expression

$$\rho(\mathbf{k}) = e^{-a\mathbf{k}^2}. \quad (7)$$

3.2 Double emission

As mentioned, the string picture is oriented towards the soft dynamics. Simultaneous emission from the string of two jets with large rapidity difference is assumed to be strongly damped. Its probability for rapidity difference $\Delta y = y_1 - y_2 > 0$ is assumed to be proportional to $\exp(-aM^2)\delta^2(k_1 + k_2)$ where $M^2 = k_{1\perp} k_{2\perp} e^{\Delta y} - 2(k_1 k_2)_\perp$ is the total mass. So it gives strong back-to-back azimuthal correlations, as for hard emissions, but they fall as $\exp(-\Delta y)$.

Long-range rapidity correlations in emission from the string may rather follow from their sequential decay into two partons.

Let us assume that after the first emission of a particle with momentum k_1 this particle forms a new string with the target from which a second emission follows producing a second particle with momentum k_2 . The total probability is obviously given by the product

$$\rho_1(k_1)\rho_2(k_1, k_2). \quad (8)$$

The initial probability is

$$\rho_1(k_1) = e^{-a\mathbf{k}_1^2} \quad (9)$$

and the second one is

$$\rho_2 k_2 = e^{a\tilde{k}_2^2}, \quad (10)$$

where \tilde{k}_2 is orthogonal to plane k_1, p_2 and given by (4) with $p = k_1 + p_2$ and $q = k_1 - p_2$. We have

$$\begin{aligned} (k_2 p) &= k_{2+}k_{1-} + k_{2-}k_{1+} + (k_2 k_1)_\perp + k_{2+}p_{2-}, \\ (k_2 q) &= k_{2+}k_{1-} + k_{2-}k_{1+} + (k_2 k_1)_\perp - k_{2+}p_{2-}, \\ p^2 &= 2k_{1+}p_{2-} = -q^2. \end{aligned}$$

So

$$\tilde{k}_2^2 = k_2^2 - \frac{(k_2 p)^2 - (k_2 q)^2}{p^2} = k_2^2 - \frac{(k_2, p+q)(k_2, p-q)}{p^2}.$$

Calculating this we have

$$\tilde{k}_2^2 = k_2^2 - 2\frac{k_{2+}}{k_{1+}}(k_{2+}k_{1-} + k_{2-}k_{1+} + (k_2 k_1)_\perp) = k_{2\perp}^2 - 2\frac{k_{2+}}{k_{1+}}(k_2 k_1)_\perp + \frac{k_{2+}^2}{k_{1+}^2}k_{1\perp}^2 = \left(k_2 - \frac{k_{2+}}{k_{1+}}k_1\right)_\perp^2.$$

So we find

$$\rho_2(k_2) = e^{a\left(k_2 - \frac{k_{2+}}{k_{1+}}k_1\right)_\perp^2}, \quad (11)$$

or in Euclidean momenta and rapidities

$$\rho_2(y_1, y_2, \mathbf{k}_1, \mathbf{k}_2) = e^{-a(\mathbf{k}_2 - e^{-\Delta y}\mathbf{k}_1)^2}. \quad (12)$$

The total probability for the double production expressed in Euclidean transverse momenta k_1 and k_2 becomes

$$\frac{dW}{dy_1 dy_2 d^2 k_1 d^2 k_2} = e^{-a(q_1^2 + q_2^2 + q_1^2 e^{-2\Delta y} - 2q_1 q_2 \cos \phi e^{-\Delta y})}. \quad (13)$$

Recall that we assume $\Delta y = y_1 - y_2 > 0$

The first two terms independent of the relative rapidity correspond to independent emission. The rest depend on the rapidity difference and exponentially fall with it. Correlations are contained in the last term. Unfortunately they again fall like $\exp(-\Delta y)$ with the rapidity distance between emitted particles.

So our conclusion is that the correlations in emissions from a single string are all of the short-range character in rapidity.

4 Long-range correlations

4.1 Correlations for given string configuration

Consider an event in which n strings are formed, which may be different. The difference may come both from the color of strings (simple or fused) and from their different location in the overlap area. The inclusive cross-section from the i -th string is $I_i(y, \phi)$. We normalize it as follows

$$\int dy d\phi I_i(y, \phi) = \langle N_i \rangle, \quad (14)$$

where $\langle N_i \rangle$ is the average number of particles emitted from string i . The total inclusive cross-section is

$$I(y, \phi) = \sum_{i=1}^n I_i(y, \phi). \quad (15)$$

Integration over y, ϕ gives the total mean number of particles, $\langle N \rangle = \sum_i \langle N_i \rangle$, emitted by the given string configuration. Note that the contribution to the sum in (15) only comes from the strings which cover rapidity y . Namely, if the upper and lower ends of the string i have rapidities y_i^u and y_i^l respectively then the contributing strings must have $y_i^l < y < y_i^u$.

Now consider the double inclusive cross-section at azimuthal angles ϕ_1 and ϕ_2 and rapidities y_1 and y_2 . We can divide all strings into three groups. Strings in the first group cover only rapidity y_1 . Strings in the second group cover only rapidity y_2 . Finally strings in the third group cover both rapidities y_1 and y_2 . The total inclusive cross-section at y_1 will be given by (15) with the sum including strings of the first and third group:

$$I(y_1, \phi_1) = \sum_i \left(I_i^{(1)}(y_1, \phi_1) + I_i^{(3)}(y_1, \phi_1) \right). \quad (16)$$

At y_2 the inclusive cross-section will come from strings of the second and third group:

$$I(y_2, \phi_2) = \sum_i \left(I_i^{(2)}(y_2, \phi_2) + I_i^{(3)}(y_2, \phi_2) \right), \quad (17)$$

Two particles at rapidities and angles y_1, ϕ_1 and y_2, ϕ_2 may come either from different strings or from the same string. In the first case the double inclusive cross-section will be given by the expression

$$\begin{aligned} I_1(y_1, \phi_1, y_2, \phi_2) &= \sum_{i,k} \left(I_i^{(1)}(y_1, \phi_1) I_k^{(2)}(y_2, \phi_2) + I_i^{(1)}(y_1, \phi_1) I_k^{(3)}(y_2, \phi_2) \right. \\ &\quad \left. + I_i^{(2)}(y_2, \phi_2) I_k^{(3)}(y_1, \phi_1) \right) + \sum_{i \neq k} I_i^{(3)}(y_1, \phi_1) I_k^{(3)}(y_2, \phi_2). \end{aligned} \quad (18)$$

In the last term the two particles come from different strings of the third group. In the second case both particles come from the same string of the third group. If we neglect correlations inside the string following the results of the preceding section then this contribution will be

$$I_2(y_1, \phi_1, y_2, \phi_2) = \sum_i I_i^{(3)}(y_1, \phi_1) I_i^{(3)}(y_2, \phi_2). \quad (19)$$

Here we have to make an important comment. Eq. (19) is true if the number of emitted particles is equal or greater than two. If it is equal to 1 then this contribution does not exist.

Neglecting this rare possibility and summing these two parts we get the total double inclusive cross-section as

$$\begin{aligned} I(y_1, \phi_1, y_2, \phi_2) &= \sum_{i,k} \left(I_i^{(1)}(y_1, \phi_1) + I_k^{(3)}(y_2, \phi_2) \right) \left(I_i^{(12)}(y_2, \phi_2) + I_k^{(3)}(y_1, \phi_1) \right) \\ &= I(y_1, \phi_1) I(y_2, \phi_2). \end{aligned} \quad (20)$$

This means that there are no correlations for events with the same string configuration.

Note that from Eq. (20) it follows that

$$J \equiv \int dy_1 d\phi_1 dy_2 d\phi_2 I(y_1, \phi_1, y_2, \phi_2) = \langle N \rangle^2. \quad (21)$$

In fact $J = \langle N(N-1) \rangle = \langle N^2 \rangle - \langle N \rangle$. But for the Poisson distribution of the particles emitted from strings $\langle N^2 \rangle = \langle N \rangle^2 + \langle N \rangle$ in accordance with (21).

4.2 Long-range correlations from fluctuating string configuration

As follows from the previous considerations, in the colour string picture correlations can arise from the superposition of many events with different number and type of strings. In fact appearance of long-range correlations in this picture was observed long ago and was considered as one of the main consequences of the string picture.

The simplest type of correlations, long discussed in literature, are the forward-backward correlations relating the probability to observe particles in the backward rapidity window with a given number of particles in the forward rapidity window. Appearance of such correlations is evident from the following reasoning. Let all the strings be equal for simplicity, If the number of strings may be different in different events, then in an event with, say, n strings the number of particles observed in the forward rapidity window is n times greater than from a single string. But in this event also the number of particles observed in the backward rapidity window will be n times greater than from a single string, so that an obvious correlation follows. This argument was later generalized to fusion and percolation of strings.

However passing to the azimuthal angle dependence one concludes that if emission from strings is isotropic, independent of their type, the correlations due to their distribution in different events will also be isotropic. Also in the central rapidity region the inclusive cross-sections are practically independent of rapidity. This generates a plateau in the $\delta y - \delta\phi$ distribution rather than a ridge, with only a narrow peak at small $\delta\phi$ and δy due to short range correlations.

This conclusion remains true if one averages the inclusive cross-sections over all events with the resulting loss of azimuthal angle dependence. So the ridge can only be obtained on the event-by-event basis.

5 Ridge and the flow coefficients

As discussed above the ridge in our picture arises due to fluctuations in both string distributions and impact parameter. So it is important to study the formation of averages relevant to the ridge.

For a particular string configuration with a fixed azimuthal angle ϕ_0 of the impact parameter the inclusive cross-section is found as a function of angle ϕ as

$$\begin{aligned} I^c(y, \phi) &= A^c(y) + 2 \sum_{n=1} \left(B_n^c(y) \cos n(\phi - \phi_0) + C_n^c(y) \sin n(\phi - \phi_0) \right) \\ &= A^c \left(1 + 2 \sum_{n=1} \left(b_n^c(y) \cos n\phi + c_n^c(y) \sin n\phi \right) \right). \end{aligned} \quad (22)$$

The flow coefficients for a given event are given by

$$v_n^c(y) = \left((a_n^c(y))^2 + (b_n^c(y))^2 \right)^{1/2}. \quad (23)$$

The experimentally observed flow coefficients are obtained after averaging over different string distributions, which we denote as $\langle \dots \rangle$

$$v_n(y) = \langle v_n(y) \rangle = \left\langle \left((a_n(y))^2 + (b_n(y))^2 \right)^{1/2} \right\rangle. \quad (24)$$

Passing to correlations, for a given string configuration we have the double inclusive cross-section given by Eq. (20):

$$\begin{aligned} &I^e(y_1, \phi_1, y_2, \phi_2) \\ &= \left(A^c(y_1) + 2 \sum_{n=1} \left(B_n^c(y_1) \cos n(\phi_1 - \phi_0) + C_n^c \sin n(\phi_1 - \phi_0) \right) \right) \\ &\times \left(A^c(y_2) + 2 \sum_{m=1} \left(B_m^c(y_2) \cos m(\phi_2 - \phi_0) + C_m^c \sin m(\phi_2 - \phi_0) \right) \right). \end{aligned} \quad (25)$$

We have to average this expression over string distributions and directions of the impact parameter ϕ_0 . The latter reduces to integration over ϕ_0 with weight $1/2\pi$. Doing first this integration and then averaging over string distribution we obtain the "experimental" double inclusive cross-section

$$I(y_1, y_2, \phi_{12}) = \langle A(y_1)A(y_2) \rangle + 2 \sum_n \langle W_n(y_1, y_2) \rangle \cos n\phi_{12}, \quad (26)$$

where $\phi_{12} = \phi_1 - \phi_2$ and

$$W_n(y_1, y_2) = B_n(y_1)B_n(y_2) + C_n(y_1)C_n(y_2). \quad (27)$$

Similar averaging of the single inclusive cross-section obviously eliminates all oscillating terms, so that

$$I(y_1) = \langle A(y_1) \rangle. \quad (28)$$

Thus we find the correlation function as

$$C(y_1, y_2, \phi_{12}) = \frac{\langle A(y_1)A(y_2) \rangle + 2 \sum_n \langle W_n(y_1, y_2) \rangle \cos n\phi_{12}}{\langle A^c \rangle^2} - 1$$

$$= \frac{DA(y_1, y_2)}{\langle A(y_1) \rangle \langle A(y_2) \rangle} + 2 \sum_{n=1} w_n(y_1, y_2) \cos n\phi_{12}, \quad (29)$$

where $DA(y_1, y_2) = \langle A(y_1)A(y_2) \rangle - \langle A(y_1) \rangle \langle A(y_2) \rangle$ is the covariance of the integrated single inclusive cross-sections, that is multiplicities, and

$$w_n(y_1, y_2) = \frac{\langle W_n(y_1, y_2) \rangle}{\langle A \rangle^2}. \quad (30)$$

As we observe the correlation contains two terms. The first is due to fluctuations in the total multiplicity and is independent of the angle. The ridge comes from the second term, which depends on averages of the product of initial coefficients B_n and C_n at different rapidities.

As mentioned, in the central region with sufficiently long strings the distributions are practically independent of rapidity. This creates a plateau in rapidity with the angular dependence of correlations given by

$$C(\phi_{12}) = \frac{DA}{\langle A \rangle^2} + 2 \sum_{n=1} w_n \cos n\phi_{12} \quad (31)$$

and

$$DA = \langle A^2 \rangle - \langle A \rangle^2, \quad w_n = \frac{\langle (B_n)^2 + (C_n)^2 \rangle}{\langle A \rangle^2}. \quad (32)$$

If one neglects fluctuations in the multiplicity at a given centrality and assumes $\langle A^2 \rangle = \langle A \rangle^2$ then one finds

$$w_n = \langle (a_n)^2 + (b_n)^2 \rangle = \langle (v_n)^2 \rangle, \quad (33)$$

that is the average of the individual flow coefficients squared. This should be compared with the normally defined flow coefficients Eq. (24), which are obtained by averaging of individual flow coefficients themselves. If fluctuations both in A and in v_n are negligible one can take $\langle (v_n)^2 \rangle = \langle v_n \rangle^2 = v_n^2$ and thus find the ridge directly from the flow coefficients.

6 Numerical calculations

6.1 AA collisions

The general scheme of calculations repeats the one presented in our previous paper dedicated to flow coefficients [22]. So here we only briefly describe the main points. A Monte-Carlo code was developed which first distributes the colliding nucleons in the transverse area according to the nuclear profile functions at a given impact parameter b . The number of interacting nucleons (participants) is determined according to the Glauber picture. Then strings are attached to participants. The number of strings per participant for a given centrality is

determined from the conclusions of [33] for energies 62.4 and 200 GeV and of [34] for the LHC energy of 2.76 TeV. Strings are assumed to fuse if they are located in a common area of radius $r_s = 0.32 fm$. The colour and tension of the string fused from n original strings are taken to be \sqrt{n} greater than for the original string. Particles are emitted from fused strings according to the thermal distribution in transverse momentum. The anisotropy of particle distribution is assumed to come from the passage of particles through the gluon field inside the strings and the corresponding quenching of their transverse momentum. As mentioned, the concrete form of this quenching is borrowed from a similar process in the quantum electrodynamics (see [31]). As a result of this Monte-Carlo code one obtains single and double inclusive cross-section in the forms (22) and (25). Averaging gives the coefficients v_n and w_n and the correlation coefficient $C(\phi)$.

Particle emission in the central region turns out to be practically independent of rapidity. So the obtained correlation coefficient corresponds to the ridge form while the rapidity distance does not become comparable with the overall rapidity. At such large rapidity distance one has to seriously take into account energy conservation and the dependence on the two rapidities y_1 and y_2 in Eq. (29).

Using the constructed Monte-Carlo code we calculated w_n for $n = 1, \dots, 16$ and then found coefficient $C(\phi)$ for energies 62.4, 200 GeV and 2.76 TeV and different centralities. The experimental data at a given centrality mostly assume multiplying $C(\phi)$ by the multiplicity minus unity:

$$C(\phi) \rightarrow \langle A \rangle C(\phi). \quad (34)$$

The resulting correlation coefficients for the above mentioned three energies are presented in Figs. 1 -3. In these figures, as in the majority of the following ones, the constant term $DA / \langle A \rangle^2$ is dropped. For AA collisions it is small (of the order of 0.1)

To illustrate the energy dependence we present the flow coefficients v_n and correlation coefficients $C(\phi)$ for all the three energies for minimum bias events in Figs. 4 and 5.

We compared our results with the experimental data for Au-Au collisions at 200 GeV presented in [6] in Fig. 6 where we show the calculated correlation coefficients $C(\phi)$ for 10% of the most central events against the experimental data from STAR.

At the LHC energy 2.76 TeV we compared our results with the data from ALICE [3] at central collisions with detected pairs of particles with rather large transverse momenta p_T between 1 and 3 GeV/c. To adjust to the average p_T we raised the minimal value of p_T for our total cross-sections to 0.5 GeV/c. The resulting correlation coefficients for most central collisions are compared with ALICE data in Fig. 7. The corresponding flow coefficients at different centralities are shown in Fig. 8 again compared to ALICE data.

As we observe, in both cases the form of our results is somewhat distorted as compared to the experimental data. We obtain a reasonable agreement with the data at angles $\leq 40^\circ$ and very good agreement at angles $\geq 110^\circ$. However the experimental data reach their minimal value around 70° , whereas the calculated values are minimal at 90° and from 40° to 100° our results lie substantially above the data. The reason of this disagreement probably has to do with simplifications made in our Monte-Carlo simulations. In fact the tension of

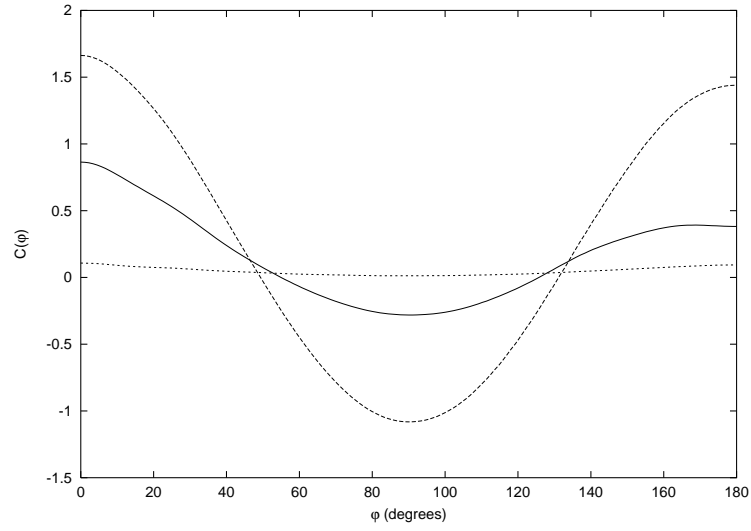


Figure 1: Correlation coefficients $C(\phi)$ for Au-Au collisions at 62.4 GeV for central(middle curve at small angles) mid-central (upper curve) and peripheral (lower curve) events

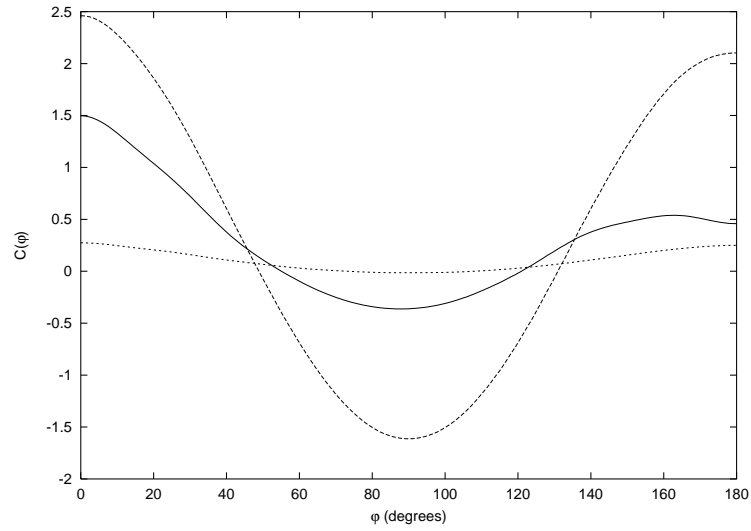


Figure 2: Correlation coefficients $C(\phi)$ for Au-Au collisions at 200 GeV for central(middle curve at small angles) mid-central (upper curve) and peripheral (lower curve) events

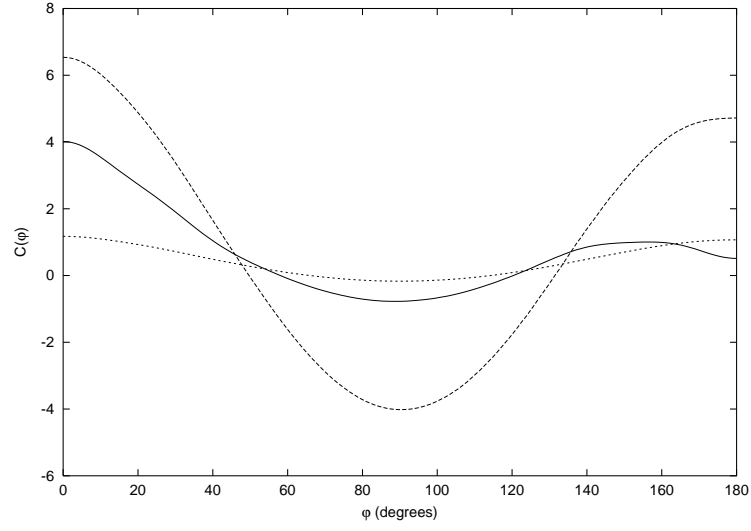


Figure 3: Correlation coefficients $C(\phi)$ for Pb-Pb collisions at 2.76 TeV for central (middle curve at small angles) mid-central (upper curve) and peripheral (lower curve) events

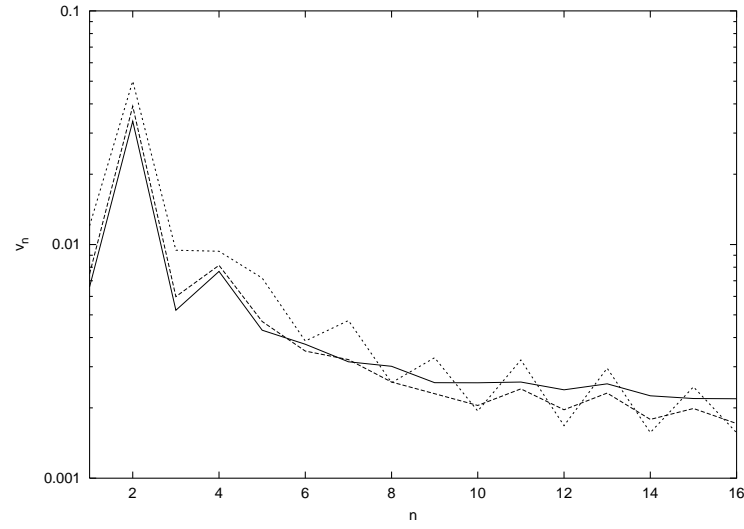


Figure 4: Flow coefficients v_n for minimum bias events in Au-Au collisions at 62.4 and 200 GeV (lower and middle curves at $n = 2$ respectively) and in Pb-Pb collisions at 2.76 TeV (upper curve at $n = 2$)

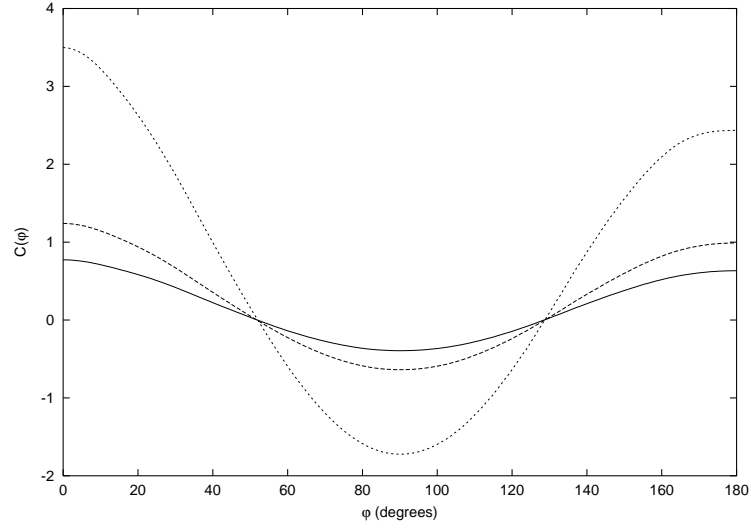


Figure 5: Correlation coefficients $C(\phi)$ for minimum bias events in Au-Au collisions at 62.4 GeV (upper curve at 90° , 200 GeV (middle curve at 90°) and Pb-Pb collisions at 2.76 TeV (lower curve at 90°)

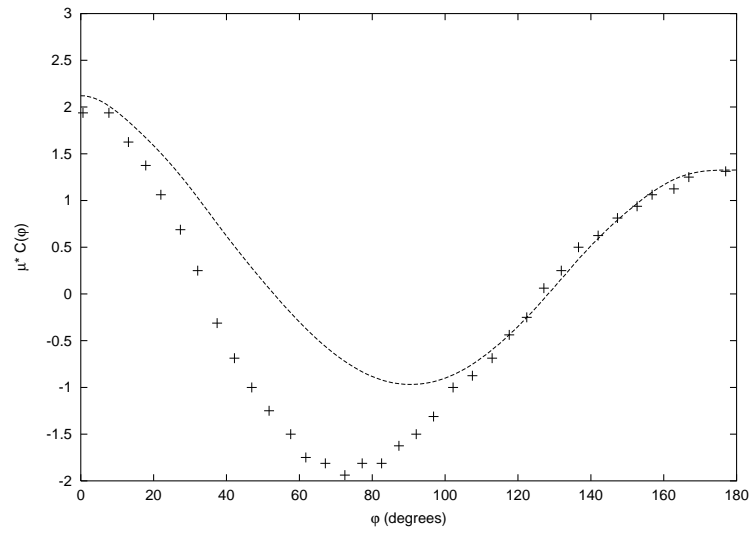


Figure 6: Correlation coefficient $C(\phi)$ for Au-Au at 200 GeV for 10% of the most central events against the experimental data from [6]

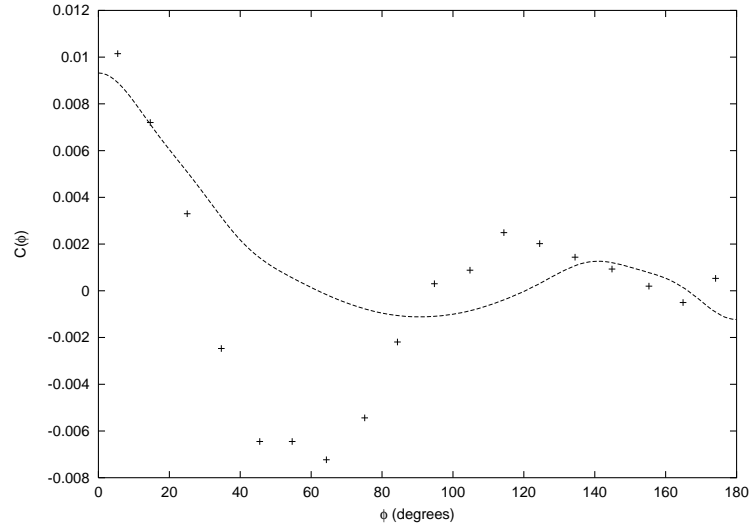


Figure 7: Correlation coefficient $C(\phi)$ for Pb-Pb at 2.76 TeV for the most central events against the experimental data from [3]

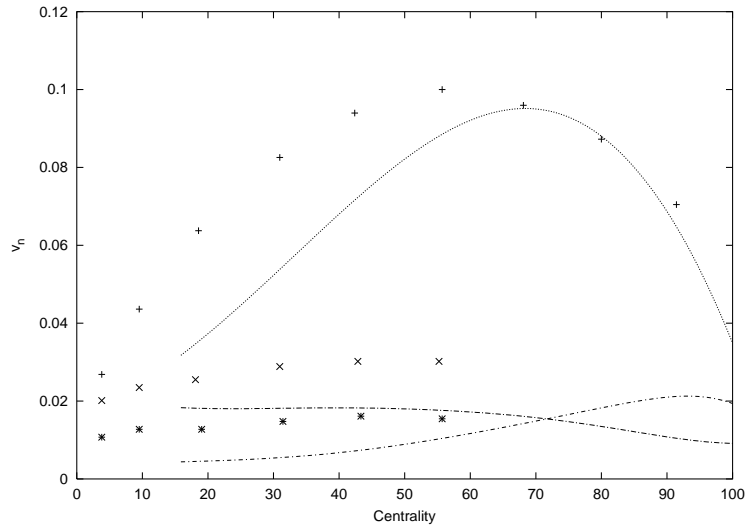


Figure 8: Flow coefficients v_2 , v_3 and v_4 (from top to bottom on the left) at different centralities for Pb-Pb at 2.76 TeV against the experimental data from [7]

a cluster of n overlapping strings is roughly $\sqrt{nS_n/S_1}$ where S_n and S_1 are areas of the cluster and simple string respectively. With that, forms of clusters with a given number of strings may be quite various. To make calculation feasible, in our Monte-Carlo code, as in ref. [22], it was assumed that all clusters have the same size and form, with the tension of each cluster just \sqrt{n} . It was previously shown that such simplification does not influence the bulk properties of the string picture, such as multiplicities and transverse momentum distribution of emitted particles. However it neglects fluctuations in the size and form of clusters and thus may distort the azimuthal asymmetry. This is especially significant for AA collisions where the total number of strings and average cluster dimension are much larger than in pp and pA collisions. This fact was already noted in [22] where we found smaller values for higher harmonics v_n , $n \geq 3$ as compared to the data for Au-Au collisions at RHIC. In pp and pA collisions the average dimension of clusters is much smaller, which may lead to better agreement with the data.

6.2 Ridge in pA collisions

In the string picture proton-nucleus collisions are described in the similar manner as for nucleus-nucleus and proton-proton collisions. The difference from the former case is that the strings are stretched between the projectile proton and all nucleons of the target at a given impact parameter b . We choose the maximal number of strings attached to the nucleons of the target to be 18 at energies in the region 5-7 TeV, in accordance with our results for the multiplicity in proton-protons collisions. The number of strings attached to the projectile proton will correspondingly be $A^{1/3}$ times larger. One might expect stronger dependence on the rapidity distance due to asymmetry between the projectile and target. However our calculations show that at least for $y_1 - y_2 \leq 4$ the results remain independent of rapidity in the central region. The resulting w_n and $C(\phi)$ are similar for energies 62.4, 200 GeV and 5.02 TeV. So we limit ourselves by presenting only our results for $C(\phi)$ at 5.02 TeV in Fig. 9. As we observe $C(\phi)$ practically do not change with centrality up to sufficiently peripheral events.

We compared our results with the data from [3] at central and peripheral collisions in Figs. 10 and 11. with the use of the ZYAM (zero-yield-at-minimum) procedure. The agreement at central collisions is quite good. At peripheral collisions our results somewhat overshoot the data. However they agree with the tendency to have smaller $C(\phi)$ at less centrality. Also our theoretical definition of centrality (the ratio of the impact parameter to its maximal value) is different from the one used in the experiment, so that our peripheral collisions are strongly contaminated by the more central collisions from the experimental point of view, which may explain comparatively large values of $C(\phi)$.

6.3 Ridge in pp collisions

In the colour string approach proton-proton collisions are described quite similarly to other hadronic processes. So we applied our Monte-Carlo simulations to calculate the flow coefficients in proton-proton collisions. From [35] one can conclude that at 62.4, 200 GeV

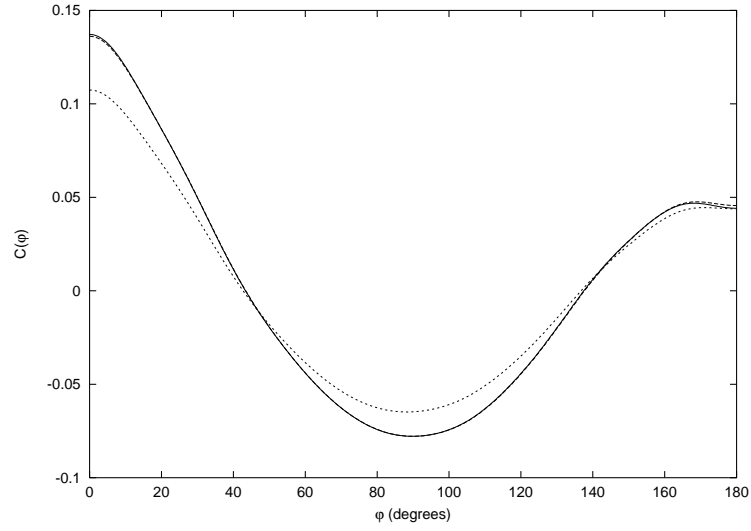


Figure 9: Correlation coefficients $C(\phi)$ for p-Pb collisions at 5.02 TeV for central and mid-central collisions (upper curve at small angles) and peripheral collisions (lower curve)

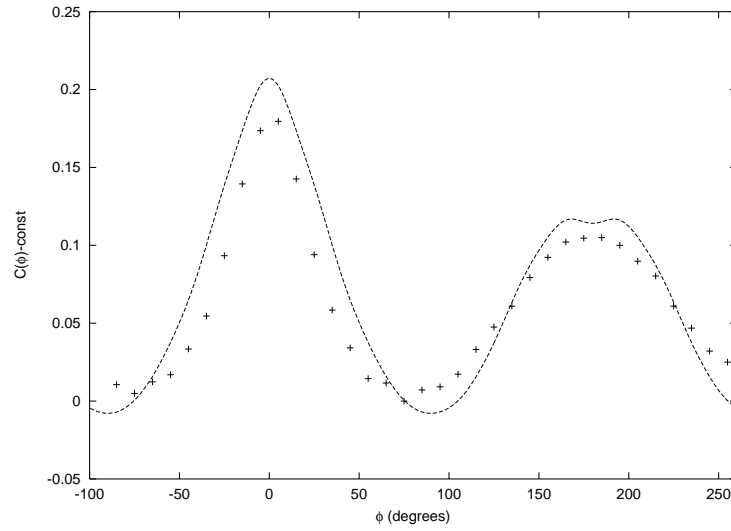


Figure 10: Correlation coefficient $C(\phi)$ for p-Pb collisions at 5.02 TeV for central collisions compared to the data in [3] (with the ZYAM procedure).

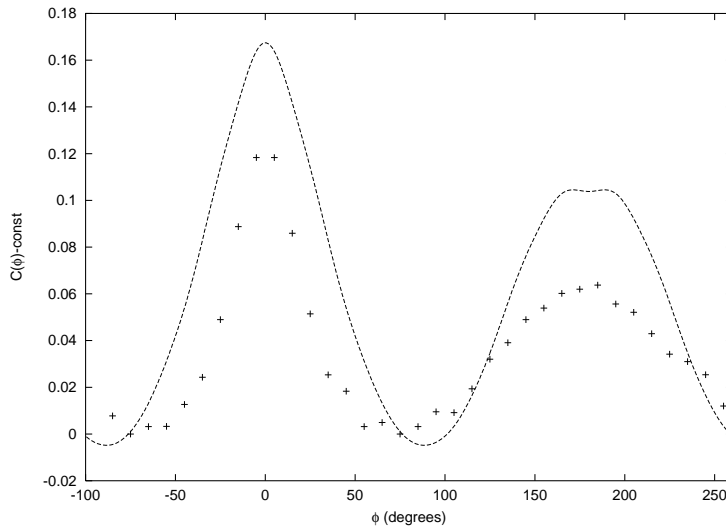


Figure 11: Correlation coefficient $C(\phi)$ for p-Pb collisions at 5.02 TeV for peripheral collisions compared to the data in [3] (with the ZYAM procedure).

and 7 TeV the average number of formed strings is 3, 4 and 9 respectively. To describe the impact parameter dependence we have assumed the distribution of hadronic matter in the proton to be a Gaussian with radius 0.8 fm. Calculations show that for such small number of strings fluctuations are quite strong, so that reliable results can be obtained after no less than 1000 simulations, in contrast to the AA case where the results are stabilized already at 100 simulations. Our results for the mentioned three energies are quite similar. So we present them only for the LHC energy of 7 TeV. The maximal number of strings corresponding to the average one is found to be 18. In Fig. 12 we show the coefficients v_n and in Fig. 13 the correlation coefficient $C(\phi)$ averaged over centralities. All the ϕ dependence is collimated to quite small angles $\phi \leq 10^\circ$. Note that in this case the constant term $DA / \langle A \rangle^2$ dropped in Fig. 13 is of the order unity, so that the ridge turns out to be only a small ripple against a constant background.

Following the experimental observations we studied a rare case in which the multiplicity is three or more times greater than the average. The maximal number of string is then found to be 50. The resulting flow coefficients v_n and correlation coefficients $C(\phi)$ are shown in Figs. 14 and 15 respectively. In the latter figure we compare our results with the experimental data from [1]. As one observes the correlation coefficient becomes quite similar to the one in AA collisions in good agreement with the experimental findings. Still the dropped constant term is again of the order unity, so that the ridge stands on a large constant pedestal.

7 Conclusions

We have analyzed the possibility to obtain the long range azimuthal-rapidity correlations (ridge) in the framework of the colour string model with fusion and percolation. An important

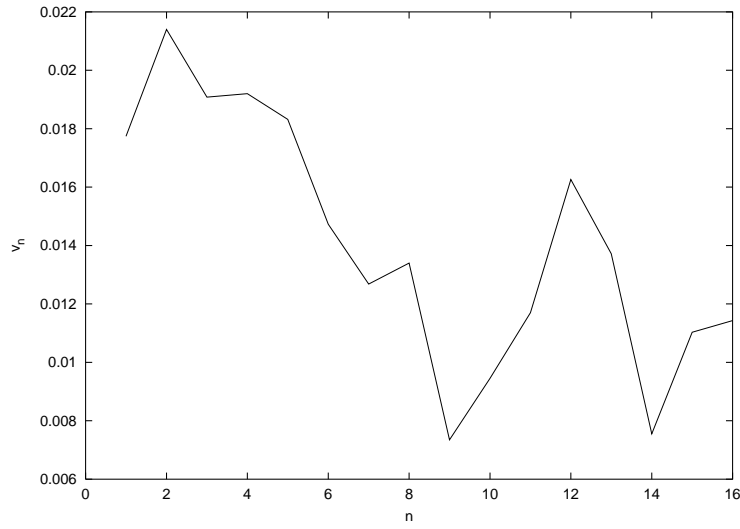


Figure 12: Flow coefficients v_n for pp collisions at 7 TeV with average multiplicity

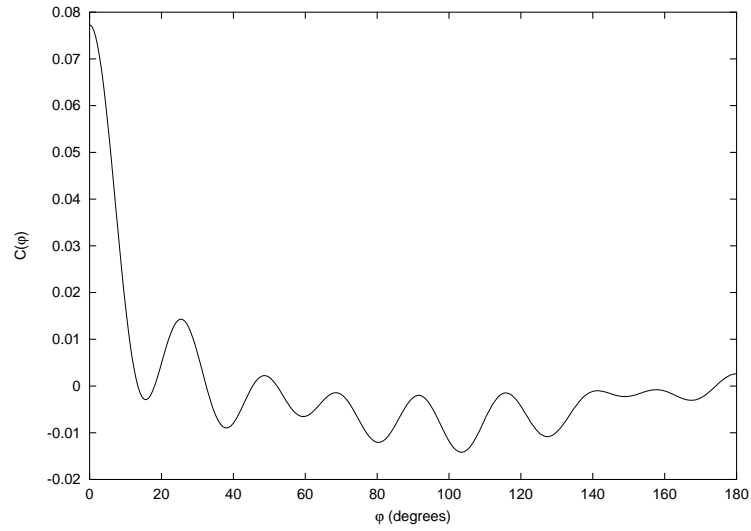


Figure 13: Correlation coefficient $C(\phi)$ for pp collisions at 7 TeV with average multiplicity

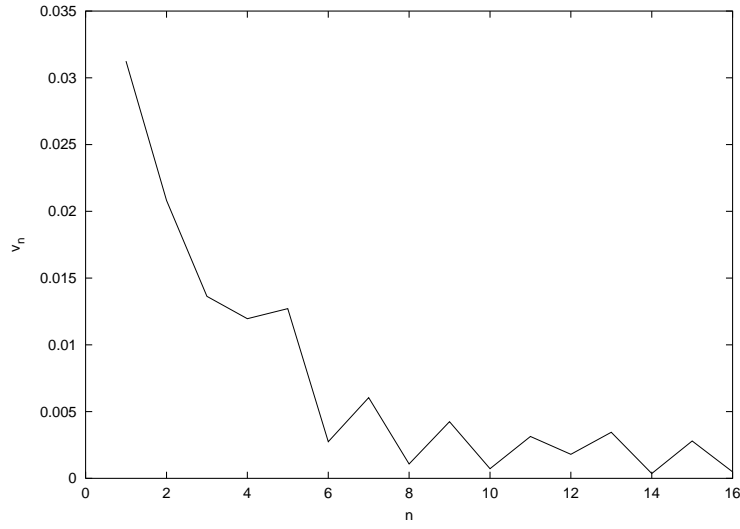


Figure 14: Flow coefficients v_n for pp collisions at 7 TeV with triple multiplicity

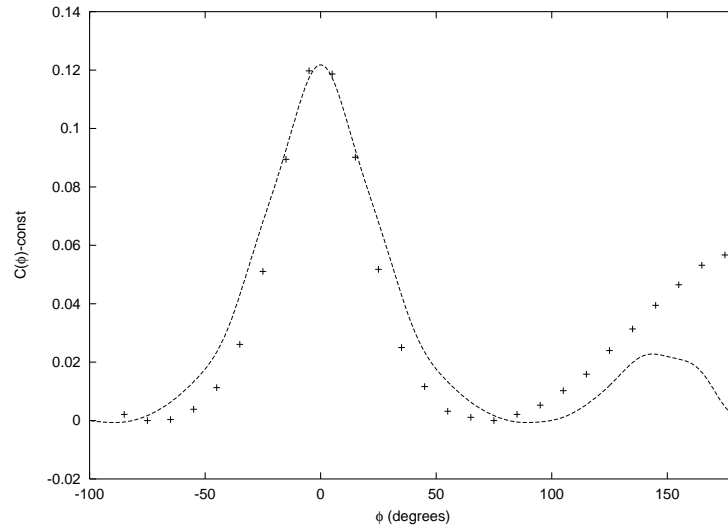


Figure 15: Correlation coefficient $C(\phi)$ for pp collisions at 7 TeV with triple multiplicity compared to the the experimental data from [1] (with the ZYAM procedure at positive ϕ)

ingredient in this approach is anisotropy of the string emission spectra in the azimuthal direction which follows from quenching of the emitted partons in the strong colour field inside the string [22]. It is found that one cannot find such correlations in a single event, since they are severely damped with the growth of the rapidity difference. Ridge can be obtained only from a superposition of many events with different numbers and types of strings. The form of ridge as a function of azimuthal difference is characterized by coefficients w_n which are generally different from the flow coefficients v_n squared and coincide with them only under certain approximations. We have performed detailed Monte-Carlo simulations to find coefficients w_n with $n \leq 16$ and found the ridge correlations in AA, pA, pp collisions at RHIC and LHC energies. The only adjustable parameter was taken from comparison with the experimental data for the elliptic flow coefficient v_2 for Au-Au minimum bias collisions at RHIC. We have confirmed that ridge appears in pp collisions only for events with an abnormally high multiplicity.

Comparing with the experimental data at RHIC and LHC we found a good qualitative agreement for angular correlations in all cases. As to the quantitative agreement it has been found to be quite good for pp and pPb collisions at 7 and 5.02 TeV, respectively. The agreement for AA collisions turned out to be reasonably good on the near side and on the away side but worse at intermediate angles where our predictions lie considerably above the data and the minimum is shifted to larger angles. The technical explanation for this may be related to smaller values for higher flow coefficients as can be seen in Fig 8. As mentioned the reason for this probably can be traced to simplifications in our Monte-Carlo simulations done to make calculations feasible. A part of fluctuations were eliminated, which may have lead to non-negligible effects especially pronounced in AA collisions. In any case it is remarkable that the ridge structure in pp, pA and AA collisions can be understood in a unified picture, at least qualitatively.

Possible refinement of our picture consists of additionally taking into account harder events, which include jet production and high-mass diffraction events. This problem is postponed for future studies.

8 Acknowledgements

M.A.B. and V.V.V. have benefited from grants RFFI 12-02-00356-a and SPbSU 11.38.197.2014 of RUSSIA, which partially supported this work. C.P. was supported by the project 2011-22776, Consolider of the Ministry of Economy of SPAIN, Xunta of Galicia and FEDER funds.

References

- [1] CMS *collab*, JHEP 1009:091, 2010; arXiv:1009.4122 [hep-ex].
- [2] CMS *collab*, Phys. Lett. **B 718** (2013) 795; arXiv:1210.5482 [nucl-ex].
- [3] ALICE *collab*, Phys. Lett. **B 719** (2013) 29; arXiv:1212.2001 [nucl-ex].

- [4] ATLAS *collab*, Phys. Rev. Lett. **110**(2013) 182302;arXiv:1212.5198 [hep-ex].
- [5] PHOBOS *collab*, Phys. Rev, **C 81** (2010) 024904 (arXiv:0812.1172); Phys. Rev. Lett. **104** (2010) 062301 (arXiv:0903.2811).
- [6] STAR *collab*, Phys. Rev. Lett **105** (2010) 022301 (arXiv:0912.3977).
- [7] ALICE *collab*,Phys. Rev. Lett., **107** (2011) 032301.
- [8] S.Gavin, L.McLerran, G.Moschelli, Phys. Rev. **C 79** (2009) 051902.
- [9] A.Dumitru, K.Dusling, F.Gelis, J.Jalilian-Marian, T.Lappi and R.Venugopalan, Phys. Lett. **B 697** (2011) 21.
- [10] S.Gavin, G.Moschelli, Phys. Rev. **C 85** (2012) 014905..
- [11] K.Dusling, T.Venugopalan, Phys. Rev. Lett. **108** (2013) 262001,(arXiv:1201.2658 [hep-ph]).
- [12] K.Dusling, T.Venugopalan, Phys. Rev. **D87** (2013) 094014, (arXiv:1302.7018 [hep-ph]).
- [13] A.Bzdak, B.Schenke, P.Triedy, R,Venugopalan, Phys. Rev. **C 87** (2013) 064906.
- [14] Yu. Kovchegov, D.E.Wertepny, arXiv:1310.6701 [hep-ph]
- [15] K.Werner, I.Karpenko, T.Pierog, Phys. Rev. Lett. **106** (2011) 122004.
- [16] E.Levin, A.Rezaeian Phys. Rev. **D 84** (2011) 034031.
- [17] A.Kovner, M.Lublinsky, Phys. Rev. **D 83** (2011) 034017; J.Mod.Phys **E 22** (2013) 1330001.
- [18] N.Armesto, L.McLerran and C.Pajares, Nucl. Phys. **A 781** (2007) 201.
- [19] N.Armesto, M.A.Braun and C.Pajares, Phys. Rev. **C75** (2007) 054902.
- [20] L.Cunqueiro, J.Dias de Deus, C.Pajares, Eur. Phys. J. **C 65** (2010) 423 (arXiv:0806.0623).
- [21] M.A.Braun, C.Pajares, Eur. Phys. J. **C 71** (2011) 1558.
- [22] M.A.Braun, C.Pajares, V.V.Vechernin, Nucl. Phys. **A 906** (2013) 14.
- [23] I.Bautista *et al*, Phys. **G 37** (2010) 015103 (arXiv:0905.3058).
- [24] N.Armesto, *private communication*.
- [25] A.Capella, U.P.Sukhatme, C.-I.Tan and J.Tran Thanh Van, Phys. Lett. **B 81** (1979), 68; Phys. Rep. **bf 236** (1994) 225.
- [26] A.B.Kaidalov and K.A.Ter-Martirosyan, Phys. Lett. **B 117** (1982) 247.

- [27] M.A.Braun and C.Pajares, Phys. Lett. **B 287** (1992) 154; Nucl. Phys. **B 390** (1993) 542,549.
- [28] J.Dias de Deus and C.Pajares, Phys. Lett. **B 695** (2011) 211.
- [29] A.Bialas, Phys. Lett. **B 466** (1999) 301.
- [30] J.Dias de Deus and C.Pajares, Phys. Lett.**B 642** (2006) 455.
- [31] A.I.Nikishov, Nucl. Phys. **B 21** (1970) 346.
- [32] A.Mikhailov, [hep-th/0305196].
- [33] T.J.Tarnowski *et al* for the STAR *collab*, Nucleonica 5183 (2006) S109-S112, arXiv:0606019 [nucl-ex].
- [34] J.Dias de Deus, A.S.Hirsch, C.Pajares, R.P.Scharenberg and B.K.Srivastava, Eur. Pgys. J **C 72** (2012) 2123, (arxiv:1106.4271 [nucl-ex]).
- [35] I.Bautista, J. Dias de Deus, J.G.Milhano, C.Pajares, Phys. Lett, **B 715** (2012) 230, (arxiv:1204.1457 [nucl-ph]).

